Crystal Structures of Neuraminidase-Antibody Complexes

W.R. TULIP,* J.N. VARGHESE,* R.G. WEBSTER,** G.M. AIR,† W.G. LAVER,‡ AND P.M. COLMAN*

*C.S.I.R.O. Division of Biotechnology, Parkville 3052, Australia; **St. Jude Children's Research Hospital, Memphis, Tennessee 38101; †Department of Microbiology, University of Alabama, Birmingham, Alabama 35294; ‡John Curtin School of Medical Research, Australian National University, Canberra 2601, Australia

The nature of antigen-antibody interactions has become clearer in the last few years as crystal structures of antigen-antibody complexes have been elucidated. Such structures have permitted a visualization of the interface between antigen and antibody. Three-dimensional structures of five complexes have now been reported, two containing the influenza virus neuraminidase as antigen and the Fabs NC41 and NC10 (Colman et al. 1987, 1989), and three with hen egg-white lysozyme and the Fabs D1.3, HyHEL-5, and HyHEL-10 (Amit et al. 1986; Sheriff et al. 1987b; E.A. Padlan et al., in prep.). The major parameters that define the scope of the antigen-antibody interface are emerging as more structures are solved and refined to greater precision. Several reviews have dealt with this topic (Mariuzza et al. 1987; Colman 1988; Davies et al. 1988).

Influenza is an orthomyxovirus and possesses an outer lipid membrane. Embedded in this membrane are two protein antigens, a hemagglutinin and a neuraminidase, the latter being a tetrameric glycoprotein comprising a head and an amino-terminal stalk that provides the attachment to the virus. Heads with full enzymatic and antigenic properties may be removed from the stalk with pronase and thus made soluble. Such heads have been used in all crystallographic investigations of the enzyme. The structure of neuraminidase of N2 subtype is known (Varghese et al. 1983) and has a structure similar to that of subtype N9 (Baker et al. 1987). N9 neuraminidase is the antigen in both of the complexes discussed here.

In this paper, we describe the crystal structure of the neuraminidase–NC41 Fab complex as refined at 2.9 Å resolution and give a structural basis for the observed lack of binding of NC41 antibody with escape mutants of N9 neuraminidase. The main features of this complex and the neuraminidase–NC10 Fab complex are also compared with those of the lysozyme complexes.

METHODS

The isolation (Laver et al. 1984) and sequencing (Air et al. 1985) of N9 neuraminidase, production of monoclonal antibodies, and properties of the neuraminidase-antibody complexes (Tulloch et al. 1986; Webster et al. 1987) have all been reported previously. Sequences of antibodies were obtained from RNA (G.M. Air, unpubl.). The crystallization and structure determination were described for complexes containing two of these antibodies, namely, NC41 (Colman et al. 1987; Laver et al. 1987) and NC10 (Air et al. 1987; Colman et al. 1989). Diffraction data sets extending to resolutions of 2.9 Å and 3.0 Å, respectively, were collected on film from a rotating anode source, and a 2.5 Å synchrotron data set was obtained for the NC41 complex. Refinement of these two crystal structures proceeded initially by the stereochemically restrained least-squares program PROLSQ (Hendrickson and Konnert 1981). In later stages, the molecular dynamics program X-PLOR (Brunger 1988) was used. The NC41 structure will be further refined against the 2.5 Å resolution data, and full details of the refinements will be presented elsewhere. Between successive rounds of refinement, the atomic models were rebuilt on an Evans and Sutherland PS300, using FRODO (Jones 1985) and displaying a $2F_o - F_c$ electron density map (where F_o is the observed structure factor and F_c is the calculated structure factor). The mean positional error of the models was estimated by a statistical method (Luzzati 1952). In the description of the structure, maximum distances for van der Waals contacts, hydrogen bonds, and salt links were as defined in Table 1 (see also Sheriff et al. 1987a). The molecular surface program MS (Connolly 1983) was used to calculate buried surface area with a probe radius of 1.7 Å. MS calculates the molecular surface area, rather than the solvent-accessible surface area (Lee and Richards 1971; Connolly 1983). Kabat numbering was used for the antibodies (Kabat et al. 1987). Amino acid residue numbers are prefixed by L (light chain) and H (heavy chain). Complementarity-determining regions (CDRs) were defined as in Kabat et al. (1987), and their sequence numbers are light chain 24–34, 50–56, and 89–97 and heavy chain 31–35, 50–65, and 95–102.

RESULTS

NC41 Complex

The R-factor ($\Sigma \| |F_o| - |F_c| \| / \Sigma |F_o|$) for 20,065 reflections from 6.0 to 2.9 Å resolution is 0.187 for the current model. Virtually all of the main-chain is observed in continuous electron density, as are most of the side-chains, but the orientations of only about half

Table 1. Contact Residues in the Interface between Neuraminidase and NC41 Fab

	NC41 Fab																			
	light chain										heavy chain									
N9 neuraminidase	Y49	W50	S52	T53	H55	I56	Y92	S93	P94	W96	N31	Y32	N52	N53	E96	D97	N98	F99	S100A	L100B
P326	·	×	·	·	·	·	·	·	·	·	·	·	·	·	·	·	·	·	·	·
R327	×	·	·	·	·	·	·	·	·	·	·	·	·	·	·	·	·	·	·	·
P328	×	·	·	×	·	·	·	·	·	·	·	·	·	·	·	·	·	·	·	·
N329	·	·	·	·	×	×	·	·	·	·	·	·	·	·	·	·	·	·	·	·
G343	·	·	·	×	·	·	·	·	·	·	·	·	·	·	·	·	·	·	·	·
N344	·	×	·	×	·	·	·	·	·	·	·	·	·	·	·	·	·	·	·	·
N345	·	·	×	·	·	·	·	·	·	·	·	·	·	·	·	·	·	·	·	·
N347	·	×	·	·	·	·	·	·	·	·	·	·	·	·	·	·	·	·	·	·
I366	·	·	·	·	·	·	·	·	·	·	×	×	·	·	·	·	·	·	·	·
S367	·	·	·	·	·	·	·	·	·	·	·	·	·	·	×	×	·	·	·	·
I368	×	·	·	·	×	·	·	·	·	·	·	·	·	·	×	·	·	·	·	·
A369	·	×	·	·	·	·	·	·	·	·	·	·	·	·	×	·	·	·	·	×
S370	·	·	·	·	·	·	·	·	·	·	·	·	·	·	·	×	·	·	·	·
S372	·	·	·	·	·	·	·	·	·	·	·	·	·	·	·	·	×	·	·	·
L399	·	·	·	·	·	·	·	·	·	·	×	·	·	×	·	·	·	·	·	·
N400	·	·	·	·	·	·	·	·	·	·	×	×	·	·	·	·	×	·	·	·
T401	·	·	·	·	·	·	·	·	·	·	·	·	×	×	·	·	×	·	·	·
D402	·	·	·	·	·	·	·	·	·	·	·	·	·	·	·	·	×	·	·	·
W403	·	·	·	·	·	·	·	·	·	·	·	·	·	·	·	·	×	×	·	·
P431	·	·	·	·	·	·	×	×	·	·	·	·	·	·	·	·	·	·	·	·
K432	·	·	·	·	·	·	·	·	×	×	·	·	·	·	·	×	·	·	×	·
D434	·	·	·	·	·	·	·	×	×	·	·	·	·	·	·	·	·	·	·	·

Residues are grouped in segments of polypeptide chain. Crosses indicate residue pairs that have at least one pair of atoms within van der Waals contact distance. Maximum contact distances (Sheriff et al. 1987a) are as follows, where C = carbon, N = nitrogen, O = oxygen: (CC) 4.107 Å; (NN) 3.441 Å; (OO) 3.33 Å; (CN) 3.774 Å; (CO) 3.719 Å; (NO) 3.386 Å. Residues partially buried from solvent by the interaction, but not in direct contact, are Thr-L31, Arg-L54, His-L91, Pro-L95, Thr-H28, Thr-H30, Gly-H33, Trp-H50, Thr-H52A, Thr-H54, Glu-H56, and Asp-H101 on the Fab, and Ile-149, Asp-330, Asn-346, Thr-396, Arg-430, Glu-433, Asp-457, Pro-459, Lys-463, and Ile-464 on the neuraminidase. In addition, two mannose residues, designated 200D and 200F, which are in the carbohydrate attached to Asn-200 of a neighboring neuraminidase subunit, are partially buried.

of the peptide carbonyl oxygen atoms are unambiguously determined in electron density at this resolution. Six water molecules were included in the model with full occupancy. The root mean square difference between ideal and observed values is 0.022 Å for bonds and 4.5° for angles, whereas the mean positional error of the atoms was estimated to be 0.3 Å.

Atoms at the interface between neuraminidase and antibody are all in convincing electron density, with the exception of side-chains in the neuraminidase segment 431–435. There appear to be no water molecules buried from solvent in the interface, but at least one water molecule is in contact with both antigen and antibody. The outline of the buried surface resembles a three-leaf clover in shape, as shown in Figure 1, with the active site in between two of the "leaves." A remarkable shape complementarity exists over most of the interface, with protuberances on one protein matched by depressions on the other. There is a large groove between the variable domains of the light and heavy chains (V_L and V_H) that accommodates a large ridge traversing the epitope made up of residues Asp-434, Lys-432, Ser-370, Ala-369, Ile-368, and Asn-329. Distances of 27 Å, 30 Å, and 27 Å separate the tips of the three parts of the interface.

Interactions between antigen and antibody include 1 salt link from Lys-432 to Asp-H97, 10 hydrogen bonds, and 115 additional van der Waals contacts, although these latter numbers may change slightly after the high-angle refinement. The buried surface area was calculated to be about 878 $Å^2$ on the surface of neuraminidase and 885 $Å^2$ on the Fab. The nonpolar (carbon and sulfur) components of the total buried surface area of neuraminidase and the NC41 variable module are 61% and 53%, respectively. These numbers are not significantly different from those of the exposed surfaces of the two proteins (58% and 59%), which implies that the epitope and paratope are not particularly hydrophobic or hydrophilic.

The epitope on neuraminidase is extensive (see Fig. 1; Table 1). It involves 5 segments on the upper surface of the enzyme, which contribute 22 residues in direct contact and 5 that are partially buried. In addition, there are partially buried atoms in 5 residues from 2 other segments and in 2 sugar residues from the carbohydrate of a neighboring subunit.

The binding site of the Fab is composed of 20 contact residues and 12 partially buried residues (see Fig. 1; Table 1). As CDR L1 is at least 5 Å from neuraminidase, only 5 of the 6 CDRs are in direct contact; as a

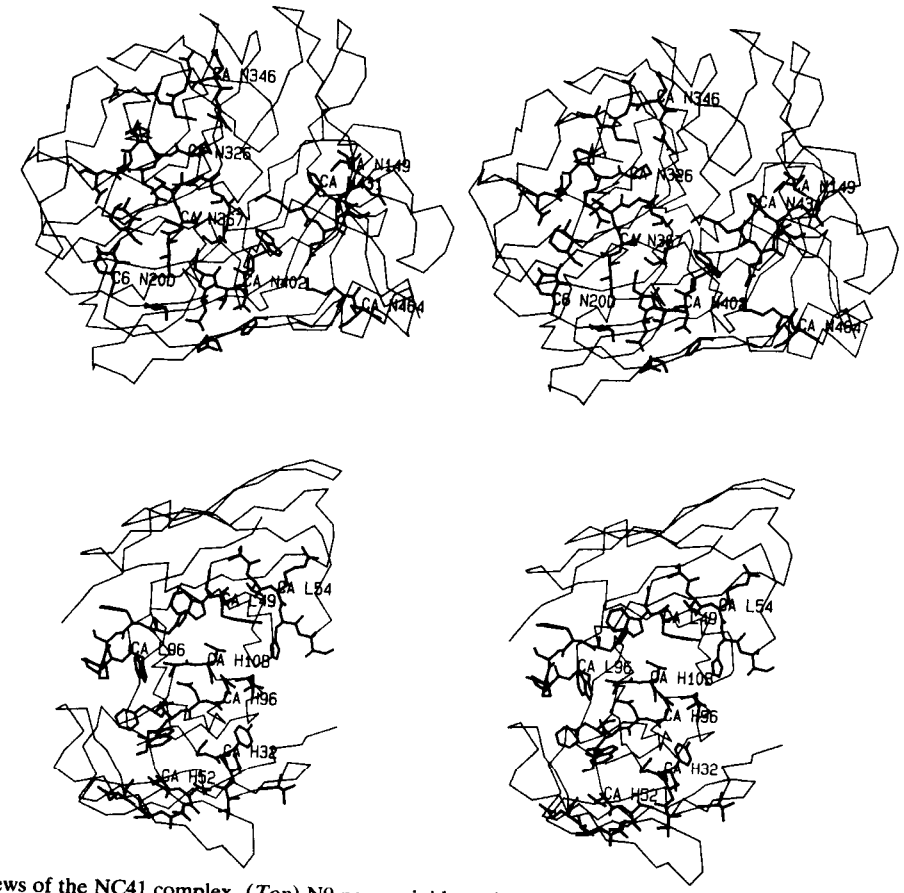

Figure 1. Stereoviews of the NC41 complex. (*Top*) N9 neuraminidase; (*bottom*) the NC41 V_LV_H dimer (light chain uppermost). The two proteins are shown opened out from a view, with the neuraminidase at left and the Fab at right, so that the interfaces are viewed *en face*. A Ca trace is drawn in thin lines for noninteracting residues. Contact and partially buried residues are shown *in toto* by bold lines. (For pairs of residues in contact, see Table 1.)

result, the heavy chain has more interaction than the light chain. The comparative data for heavy and light chains, respectively, are 506 Å^2 and 383 Å^2 for the buried surface area; 6 and 5 for the number of ion pairs and hydrogen bonds; and 72 and 43 for the number of other contacts. Among the hypervariable loops, CDR H3 has the most buried surface area (267 Å^2), representing 30% of the total, and it also has the greatest number of contacts (60). There are three framework region (FR) residues in the paratope, namely, Tyr-L49, Thr-H28, and Thr-H30, all of which are in segments adjacent to CDRs.

Possible Conformational Changes in Antigen and Antibody

Colman et al. (1987) reported that the structure of both the antigen and NC41 antibody may have changed as a result of antibody binding (for review, see Colman 1988). The refinement of the NC41 complex is essentially complete, whereas the refinement of uncomplexed N9 neuraminidase (Baker et al. 1987) at 2.2 Å resolution has not yet converged. A detailed comparison of the free and liganded neuraminidase structures will be possible in the near future. On the other hand, the structure of the free Fab has not been determined; hence, there can be no direct comparison with the uncomplexed antibody. Comparisons with other Fab structures may suggest possibilities.

At the level of local change, it appears that the main-chain conformations of five CDRs follow the canonical structures as predicted (Chothia and Lesk 1987; C. Chothia et al., in prep.). Hence, the local fold of each of these five loops is unlikely to have changed substantially upon the formation of a complex. However, CDRs can be flexible, for example, CDR L1 in Fab McPC603 (Satow et al. 1986) and CDR H3 in Fab 19.9 (Lascombe et al. 1989). As the Fab engages antigen, structural rearrangements might take place in both proteins. Such changes could be similar to those seen in the regions of crystal contacts (Wlodawer et al. 1987) or in enzyme-inhibitor interactions (Greenblatt et al. 1989).

On the basis of observed variability in V_LV_H interactions in antibodies (Davies and Metzger 1983), it has been suggested that antigen might cause small rearrangements in the V_LH_H interface (Colman et al. 1987). Whether or not this has happened in the NC41 complex remains unclear. The analysis of that complex showed that its V_LV_H pairing was an outlier among other uncomplexed Fab structures. The angular differences in the V_LV_H pairing (see Table 1 in Colman et al. 1987) of NC41 relative to New, McPC603, Kol, and J539 are currently 7.4°, 7.7°, 10.3°, and 11.5°. Given that such differences of up to 12.8° have since been found between uncomplexed Fabs (Lascombe et al. 1989), NC41 can no longer be considered as an outlier. Direct evidence for this putative quaternary change can

plexed antibodies. A reported rotation of the side-chain of Trp-H47 (Colman et al. 1987) has not been substantiated by the structure refinement. That tryptophan now appears to have a canonical structure.

Escape Mutants of N9 Neuraminidase

Monoclonal antibodies directed against neuraminidase have selected a number of escape mutants of N9 (see Tables 2 and 3 in Webster et al. 1987). Nine different mutants have been so selected, eight of them possessing single-site sequence changes in the contact surface with NC41. Figure 2 shows the positions of the nine mutants on a schematic diagram of neuraminidase. Several of these mutants crystallize isomorphously with wild-type N9, and their structures are being analyzed. Two, in particular, Ox1 (370 Ser→Leu) and Ox2 (329 Asn→Asp), have now been studied by difference Fourier methods, and preliminary results indicate local changes only for the Ox1 substitution, and no structural change associated with the Ox2 substitution.

The possible effect of the nine substitutions on the binding of NC41 antibody can be considered now that the structure of the interface is known in detail. The inhibition of neuraminidase activity by NC41 antibody was measured for these nine substitutions (see Fig. 2 in Colman et al. 1987). Wild-type neuraminidase is inhibited, but there is no loss of activity for most of the mutants, indicating that the mutation has lowered the binding affinity of NC41. A decrease in activity, as a result of antibody binding, could be explained by two mechanisms. First, the access of substrate to and/or release of product from the enzyme's active site may be sterically hindered. Second, the active site could be

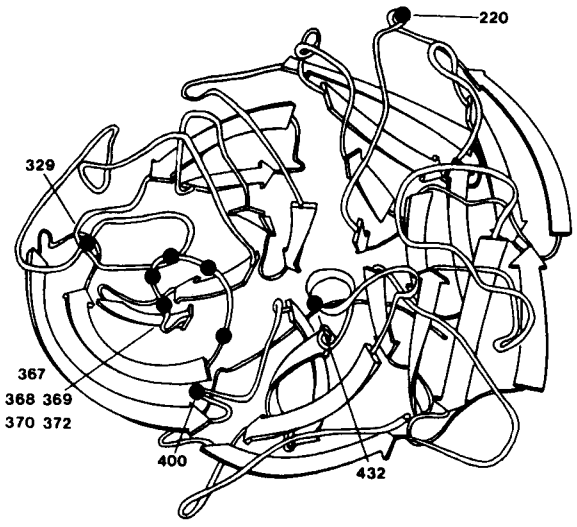

Figure 2. Schematic diagram of one of the four subunits of neuraminidase viewed down the molecular fourfold rotation axis (*bottom right*). Arrows represent β-sheet strands. Sites of mutation in N9 neuraminidase are numbered. All of the mutations except 220 occur at residues that lie in the epitope

deformed statically or dynamically. Recent studies (J.N. Varghese, unpubl.) have shown the orientation of sialic acid in the active site, which implies that the approach of substrate into the site requires the aglycon part of the substrate to be in the vicinity of the epitope recognized by NC41.

Six of the nine substitutions replace smaller side chains by larger ones, namely, 367 Ser→Asn, 368 Ile→Arg, 369 Ala→Asp, 370 Ser→Leu, 372 Ser→Tyr, and 400 Asn→Lys. All of these substitutions would be expected to diminish the shape complementarity of the antigen-antibody interface leading to low binding affinity, and the results indicate that this is true for all but the 368 substitution, designated NC24V1. Ile-368 is spatially near the middle of the epitope, and yet the mutation has little effect on the binding of NC41. An inspection shows that it is sitting at the base of a solvent-accessible pocket, which has both Fab and neuraminidase residues on its sides, and that an arginine side-chain could be accommodated if it followed the CG2 path of the isoleucine. This would first entail the loss of contacts made by CG1 and CD1 of the isoleucine and the creation of a hole where those two atoms were, and then the possible disturbance of other interacting residues by the arginine side-chain, such as Asn-329 and mannose-200F. Tentative support for such a placement of the arginine side-chain is given by a difference Fourier with (F_{obs}NC24V1 − F_{obs}Nati) as coefficients, but the data are sparse and only extend to 3.8 Å resolution.

One mutant, 432 Lys→Asn, involves a decrease in the size of the side-chain, and although this would not produce a clash as above, the inhibition result indicates that the affinity of NC41 for that mutant is very low. This is not surprising because two good contacts (< 3.0 Å) and two ordinary contacts (< 3.9 Å) would be lost, including the only ion pair in the interface. The charge on Asp-H97 would then be unbalanced, even if a water molecule were bound in the hole.

The only mutant that potentially preserves the shape complementarity but changes the chemical complementarity of the epitope is 329 Asn→Asp, designated Ox2. Its neuraminidase activity is decreased, indicating that NC41 does bind to Ox2 but not as strongly as to wild type. The complex between Ox2 and NC41 Fab crystallizes isomorphously to wild type, and a data set has been collected from the crystals, but the model has not as yet been refined against it. A difference map of the wild-type complex with the Ox2 complex confirms our earlier conclusion (Colman et al. 1987) that the binding of the antibody to these two antigenically distinct neuraminidases is isoteric. An X-ray refinement of the mutant complex is needed to confirm and clarify any small structural rearrangements that may be a consequence of accommodating the aspartate at 329 in the interface.

NC10 Complex

At this stage, the refinement has not progressed significantly since the structure was reported (Colman et al. 1989). The R-factor for 12,674 reflections in the resolution range 6.0–3.0 Å is 0.20, but segments of chain still remain out of density. In particular, the details of the interface, including buried surface area and numbers of contacts, are not clear. Nevertheless, it is apparent that the epitopes recognized by NC10 and NC41 are largely overlapping (Colman et al. 1989). In addition, the mode of attachment of the two antibodies is completely different. As shown in Figure 3, the

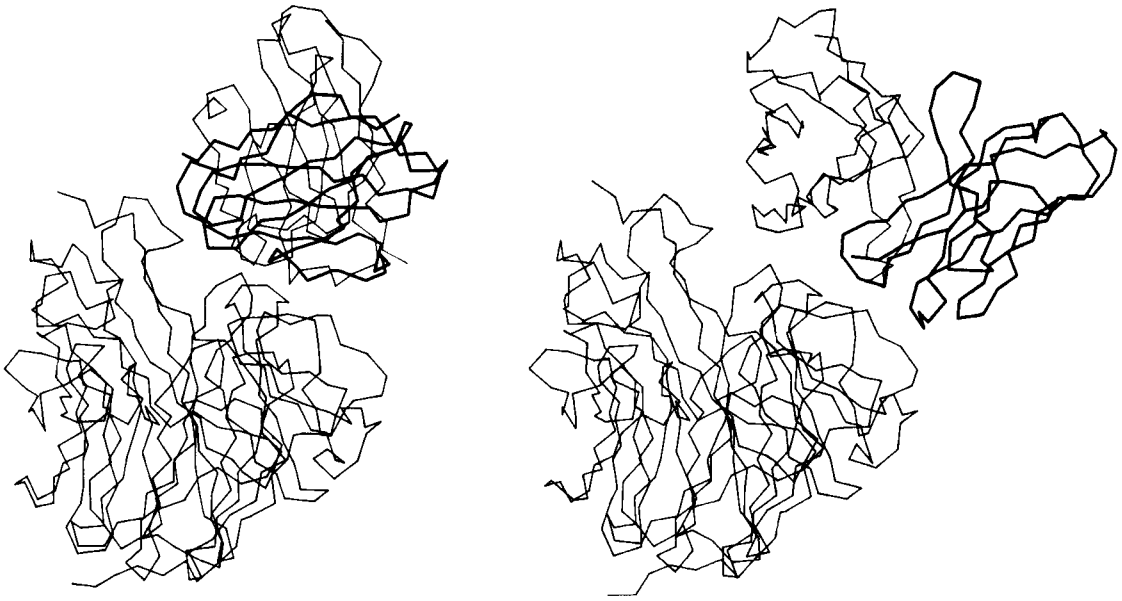

Figure 3. (*Left*) The tern N9 neuraminidase–NC41 Fab complex; (*right*) the whale N9 neuraminidase–NC10 Fab complex. On both diagrams, the neuraminidase (*lower left*) and the $V_L V_H$ dimer (*upper right*) are shown, with the neuraminidases in the same orientation. Ca traces of neuraminidase and heavy chains are indicated by thin lines, and light chains, by bold lines.

DOCKET ALARM

Explore Litigation Insights

Docket Alarm provides insights to develop a more informed litigation strategy and the peace of mind of knowing you're on top of things.

Real-Time Litigation Alerts

Keep your litigation team up-to-date with **real-time alerts** and advanced team management tools built for the enterprise, all while greatly reducing PACER spend.

Our comprehensive service means we can handle Federal, State, and Administrative courts across the country.

Advanced Docket Research

With over 230 million records, Docket Alarm's cloud-native docket research platform finds what other services can't. Coverage includes Federal, State, plus PTAB, TTAB, ITC and NLRB decisions, all in one place.

Identify arguments that have been successful in the past with full text, pinpoint searching. Link to case law cited within any court document via Fastcase.

Analytics At Your Fingertips

Learn what happened the last time a particular judge, opposing counsel or company faced cases similar to yours.

Advanced out-of-the-box PTAB and TTAB analytics are always at your fingertips.

API

Docket Alarm offers a powerful API (application programming interface) to developers that want to integrate case filings into their apps.

LAW FIRMS
Build custom dashboards for your attorneys and clients with live data direct from the court.

Automate many repetitive legal tasks like conflict checks, document management, and marketing.

FINANCIAL INSTITUTIONS
Litigation and bankruptcy checks for companies and debtors.

E-DISCOVERY AND LEGAL VENDORS
Sync your system to PACER to automate legal marketing.